



# Pharmacological Analysis of Intrinsic Neuronal Oscillations in *rd10* Retina

Sonia Biswas<sup>1</sup>, Christine Haselier<sup>2</sup>, Anja Mataruga<sup>1</sup>, Gabriele Thumann<sup>2\*</sup>, Peter Walter<sup>2</sup>, Frank Müller<sup>1\*</sup>

**1** Institute of Complex Systems, Cellular Biophysics, ICS-4, Forschungszentrum Jülich GmbH, Jülich, Germany, **2** Department of Ophthalmology, RWTH Aachen University, Aachen, Germany

## Abstract

In the widely used mouse model of retinal degeneration, *rd1*, the loss of photoreceptors leads to rhythmic electrical activity of around 10–16 Hz in the remaining retinal network. Recent studies suggest that this oscillation is formed within the electrically coupled network of AII amacrine cells and ON-bipolar cells. A second mouse model, *rd10*, displays a delayed onset and slower progression of degeneration, making this mouse strain a better model for human retinitis pigmentosa. In *rd10*, oscillations occur at a frequency of 3–7 Hz, raising the question whether oscillations have the same origin in the two mouse models. As *rd10* is increasingly being used as a model to develop experimental therapies, it is important to understand the mechanisms underlying the spontaneous rhythmic activity. To study the properties of oscillations in *rd10* retina we combined multi electrode recordings with pharmacological manipulation of the retinal network. Oscillations were abolished by blockers for ionotropic glutamate receptors and gap junctions. Frequency and amplitude of oscillations were modulated strongly by blockers of inhibitory receptors and to a lesser extent by blockers of HCN channels. In summary, although we found certain differences in the pharmacological modulation of rhythmic activity in *rd10* compared to *rd1*, the overall pattern looked similar. This suggests that the generation of rhythmic activity may underlie similar mechanisms in *rd1* and *rd10* retina.

**Citation:** Biswas S, Haselier C, Mataruga A, Thumann G, Walter P, et al. (2014) Pharmacological Analysis of Intrinsic Neuronal Oscillations in *rd10* Retina. PLoS ONE 9(6): e99075. doi:10.1371/journal.pone.0099075

**Editor:** Erica Lucy Fletcher, The University of Melbourne, Australia

**Received:** December 18, 2013; **Accepted:** May 11, 2014; **Published:** June 11, 2014

**Copyright:** © 2014 Biswas et al. This is an open-access article distributed under the terms of the Creative Commons Attribution License, which permits unrestricted use, distribution, and reproduction in any medium, provided the original author and source are credited.

**Funding:** This work was supported by the Deutsche Forschungsgemeinschaft (www.dfg.de) (grants TH 603/15-1 to GT, WA 1472/6-1 to PW, MU 3036/3-1 and MU 3036/2-1 to FM). The funders had no role in study design, data collection and analysis, decision to publish, or preparation of the manuscript.

**Competing Interests:** The authors have declared that no competing interests exist.

\* E-mail: f.mueller@fz-juelich.de

‡ Current address: Département des neurosciences cliniques, Service d'ophtalmologie, Hôpitaux universitaires de Genève, Genève, Switzerland

## Introduction

Retinitis pigmentosa (RP) is a genetically heterogeneous disease that leads to photoreceptor death associated with constriction of the visual field and, ultimately, blindness. A common reason for RP in humans is a mutation in the gene encoding the  $\beta$ -subunit of the rod phosphodiesterase (PDE). Similar mutations also exist in mouse, providing suitable animal models to investigate the course of retinal degeneration as well as therapeutic approaches.

Mouse models of retinal degeneration are indispensable tools to explore the mechanisms of degeneration as well as experimental therapies for the currently not treatable human RP. The most commonly used mouse model for RP is the *rd1* mouse [1–3]. In retinae of *rd1* mice, pronounced degeneration of photoreceptors starts around postnatal day 8 (P8). By three weeks of age, rods are completely lost [4,5]. Cones also degenerate, albeit at a slower pace. Photoreceptor death leads to a total loss of the outer part of the retina, while the inner retinal part encompassing bipolar cells, horizontal cells, amacrine cells, and ganglion cells persists. However, recently evidence has accumulated that the death of photoreceptors leads to secondary remodelling of neurons in the inner retina. Remodelling includes loss or sprouting of neuronal processes, cell migration and reactive gliosis [6–9]. The fast degeneration in *rd1* mice is a major drawback of the model. Rod degeneration starts while the retina is still in the process of differentiation. Pathological processes observed in *rd1* retinae

could, therefore, result from degeneration, a disturbed differentiation, or a mixture of both.

An alternative to *rd1* is the *rd10* mouse. These animals display a mutation in the same gene; however, the onset of photoreceptor degeneration is delayed. In *rd10* mice, rods start to degenerate after P16. By this time, all retinal layers and cell types as well as synaptic connections have been established and the major phase of retinal differentiation is over. Maximal cell death occurs between P21 and P25. By P60, only cones have survived. Hence, *rd10* mice mimic the disease process in human RP more accurately than *rd1* mice [10,11].

Currently, there is no treatment for RP. However, the persistent inner retina provides a target for therapies. One possibility is driving retinal activity via electrical stimulation by neural prostheses or optical stimulation using ectopically expressed light sensitive proteins. In these attempts to restore vision, success crucially depends on the functional integrity of the remaining retinal ganglion cells and their ability to reliably transmit visual signals to the brain. In both *rd1* and *rd10*, spontaneous rhythmic electrical activity was observed in both ganglion cell spiking and in local field potentials recorded using multi electrode arrays (MEAs). The origin of this rhythmic electrical activity is not entirely clear. In *rd1* retinae, there is evidence that cone bipolar cells and AII amacrine cells may be involved [12]. However, while in *rd1* rhythmic activity displays frequencies in the range of 10–16 Hz, in

*rd10* frequencies are lower [13–17]. Moreover, as the degeneration process differs between *rd1* and *rd10*, rhythmic activity might have different origins in both retinal models. It is important to understand the mechanisms and the properties of the rhythmic electrical activity as it may degrade the signal to noise ratio and may reduce the clarity of information transmission from eye to the brain. In the present study, we investigated the properties of rhythmic activity in *rd10* retinæ using a pharmacological approach.

## Results

### Immunohistochemistry

The degeneration of the outer retina, the changes in retinal thickness, and the retinal remodeling occurring in *rd10* mice have been analyzed by several groups using immunohistochemical stainings of vertical sections of different postnatal stages [10,11]. Our immunohistochemical analysis in principle confirmed these recently published data. Although we carefully analyzed various postnatal stages (P6, P14, P20, P25, P32, P45, P60, and 6 months) using a variety of antibodies, only few stainings are shown in Fig. 1. In many instances we visualized proteins whose expression level differs strongly between different cell types or between different compartments of one cell, e.g. processes and soma. In order to visualize degeneration induced changes in the delicate and weakly labeled processes, sometimes saturation of the strongly stained structures (e.g. somata) had to be accepted. However, for each staining identical settings were chosen for wild type retina and *rd10* retina.

As published by others [10,11] we observed an ongoing reduction in the number of photoreceptor cell layers in the ONL during maturation of the *rd10* retina (data not shown). While up to 12 rows are typical for an adult wild type retina and can still be found in *rd10* mice at postnatal stage 20, only up to 3 rows are detectable at P25. At P32, only one to two rows of somata in the ONL remained. In adult wild type retina, the antibody against red/green opsin stains numerous cone outer segments in the OS (Fig. 1A). In *rd10* retina (B) the morphology of these outer segments is clearly aberrant (arrowhead) and their number is considerably reduced.

In *rd10* retina at P32, the remaining photoreceptors are still highly immunoreactive for recoverin (D), similar as in wild type retina (C). In mouse retina, the antibody against recoverin also labels type 2 cone bipolar cells, albeit much weaker than photoreceptors [18]. As described earlier, the inner retinal cell types seem to be less affected in *rd10* mice than the outer retinal cells [10,11]. At P32, we found intact type 2 cone bipolar cells that stratify in the correct sublamina of the IPL. At later stages however, somata were sometimes displaced and dendrites were missing (data not shown).

Compared to adult wild type mouse retina (E), rod bipolar cells of *rd10* mice stained with the antibody against PKC $\alpha$  (F) showed no obvious alteration in their somata, axons, and terminal systems. However, due to the ongoing degeneration of rod photoreceptors, rod bipolar cells revealed a clear reduction of their dendrites. At P32, most of the rods are already degenerated [11] and the loss of most of the rod bipolar cell dendrites in the OPL becomes obvious (compare inserts in E and F, arrowhead in E). Furthermore, some of the rod bipolar somata were located to an aberrant position between ONL and OPL (F, arrowhead).

In wild type, the antibody against mGluR6 stained two morphologically distinct structures. By double labeling with antibodies against PKC $\alpha$  (data not shown but see references) the cloud of fine puncta spreading from the OPL into the first row of

somata in the ONL can be identified as dendritic tips of rod bipolar cells (punctate staining in G, arrowhead) [19,20]. By double labeling with peanut agglutinin (data not shown) the mGluR6 positive dendritic tips of cone bipolar cells invaginating the cone pedicles can be identified [20]. As the dendritic tips are densely packed, at this magnification puncta merge into a flat continuously stained structure (arrow, G). In *rd10* P32 retinæ, most of the punctate staining originating from rod bipolar dendritic tips had disappeared while mGluR6 at cone pedicles could still be observed. Moreover, mGluR6 staining had spread over the somata and axonal compartments of ON-bipolar cells (H).

Antibodies against calbindin stain the only horizontal cell type present in the mouse retina [21]. The somata of horizontal cells are located in the outermost row of the INL close to the OPL. While Gargini and co-workers [11] reported only slight changes in horizontal cells in *rd10*, more pronounced changes were described by Phillips and co-workers [10]. We, therefore, looked at changes in horizontal cells in more detail. At P32 we sometimes observed abnormally formed and misplaced horizontal cells in *rd10* retinæ. In the example shown in Fig. 1J, the somata of some horizontal cells were shifted towards the middle of the INL (arrowhead). Compared to wild type (I, inset) the CabP-positive processes in the OPL were clearly reduced at P32 (J, inset) as most of the photoreceptors had disappeared at this stage. At later stages, sprouting of ectopic processes was regularly found in horizontal cells (Fig. 1K), confirming the report of Phillips et al. [10]. The much weaker stained CabP-positive amacrine cells in the INL and displaced amacrine cells in the GCL were found in wild type as well as in *rd10* retina. This was also true for the three fine layers in the IPL which are formed by the stratification of ON- and OFF-cholinergic and nitric oxide synthase-positive amacrine cells [22]. Thus, the general architecture of the inner retina, especially the IPL, barely seems to be changed at P32, but may be affected at later stages (Fig. 1K).

### Retinæ of *rd10* Mice Display Spontaneous Rhythmic Activity

We recorded spontaneous electrical activity from isolated *rd10* retinæ of adult animals (P30–P360) using multi-electrode arrays. Fig. 2A shows a typical recording from one electrode displaying two different signal components (age of animal 12 months). First, fast voltage changes reflect extracellularly recorded action potentials of retinal ganglion cells that can be isolated using appropriate filter settings (Fig. 2B, high pass filter setting 300 Hz). In the lower frequency range (Fig. 2C, low pass filter setting 50 Hz) voltage modulations can be observed also known as slow wave components [15]. These local field potentials (LFPs) reflect changes in the extracellular ion composition that accompany neuronal activity. Oscillations in the LFPs were observed regularly in *rd10* retinæ, but were never recorded from wt retinæ under these experimental conditions (data not shown).

Ganglion cell spiking patterns could vary from cell to cell. In many instances, rhythmic ganglion cell spiking was observed. The recording in Fig. 2A - C displays spikes from at least two ganglion cells. The spikes with large amplitudes were fired in very short bursts that were phase locked to the minima of LFPs, while the spikes with smaller amplitude were more evenly distributed (Fig. 2B, filtered data). As displayed in Fig. 2D - F from another recording (age of animal 9 months), spikes could also appear phase locked to other phases of LFPs. In this example, spikes were not fired as short bursts but rather in groups of 3–4 spikes during the positive-going or flat component of the LFP.

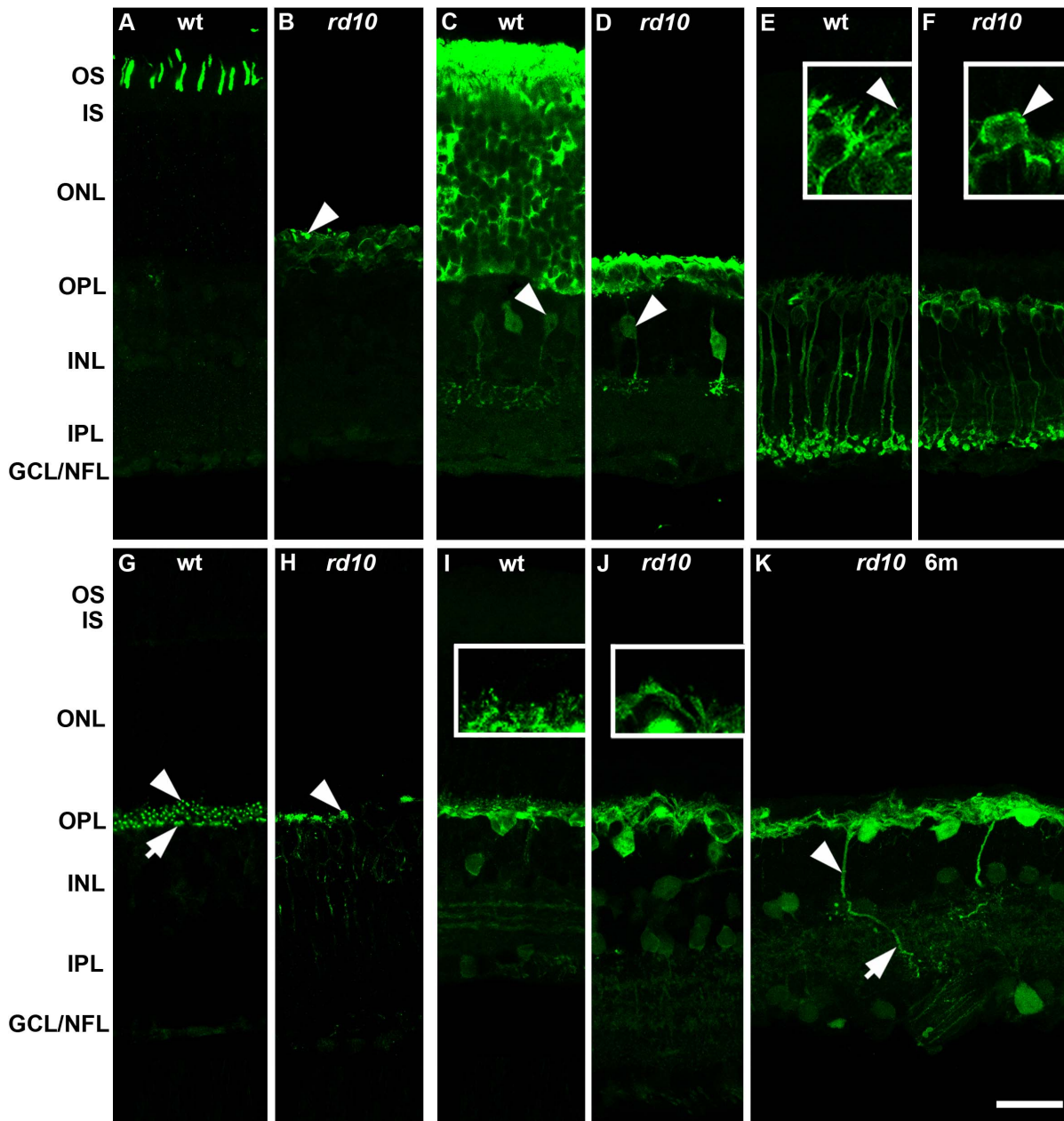


**Figure 1. Comparison of confocal images of immunohistochemically stained vertical sections through the retinas of wild type mice (wt) and *rd10* mice.** Stainings against red/green opsin (A, B), recoverin (C, D), PKC $\alpha$  (E, F), mGluR6 (G, H), and calbindin (I, J, K). With the exception of K, stainings of *rd10* retina are displayed at postnatal day 32 (P32). In contrast to wt (A) staining for red/green opsin in *rd10* was found in very few shortened outer segments (B, arrowhead) and somata of degenerating cone photoreceptors. The expression of recoverin in remaining photoreceptors and in type 2 cone bipolar cells of *rd10* (D) seemed to be unaffected compared to wt (C). In wt (E) rod bipolar cells were labeled with antibodies against PKC $\alpha$  (arrowhead indicates dendritic processes). In *rd10* (F) nearly all rod bipolar cell dendrites were lost at P32. Some PKC $\alpha$ -positive somata were displaced towards the outer retina (F, arrowhead). In wt (G) mGluR6 immunoreactivity was found as individual puncta (rod bipolar cell dendritic tips, arrowhead) and as condensed puncta at cone pedicles (cone ON-bipolar cell contacts, arrow). In *rd10*, only cone ON-bipolar cell contacts were detectable at P32 (H, arrowhead). In comparison to wt (I), horizontal cells in *rd10* retina extend much fewer fine dendrites (compare I and J, insets). Some horizontal cell bodies become displaced during degeneration (J, arrowhead). Ectopic processes of horizontal cells can be pronounced at later stages of degeneration (K, postnatal month 6). OS, outer segments; IS, inner segments; ONL, outer nuclear layer; OPL, outer plexiform layer; INL, inner nuclear layer; IPL, inner plexiform layer; GCL, ganglion cell layer; NFL, nerve fibre layer. Scale bars 25  $\mu$ m for overviews and 10  $\mu$ m for insets.  
doi:10.1371/journal.pone.0099075.g001

Electrical activity recorded from *rd10* retinas differs strongly from that found in wt retinas, but is reminiscent of the electrical activity observed in *rd1* retinas. However, peaks in the LFPs occur at different frequencies. While in *rd1*, frequencies of 10–16 Hz

were observed [14,16,23], we and others [16] mostly found basic frequencies of 3–4 Hz in *rd10*. In some cases, we also observed frequencies of 5–6 Hz in *rd10* retinas (see Fig. S1). In most instances, Fourier analysis revealed peaks with second or even

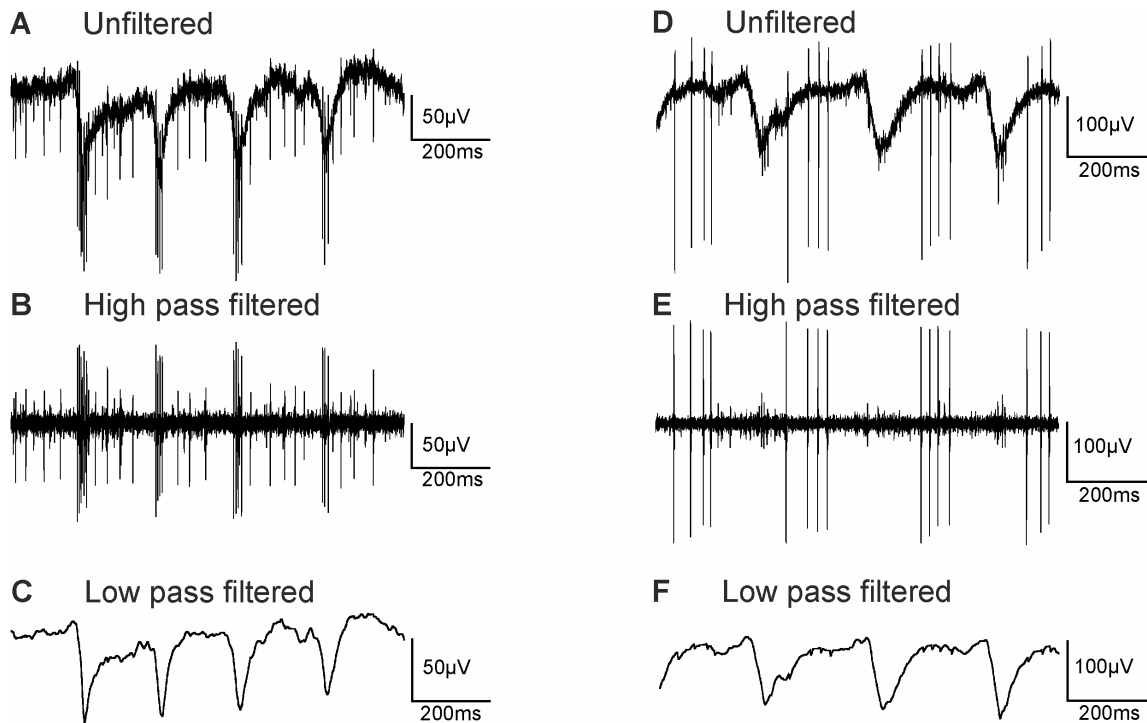


**Figure 2. Rhythmic activity is observed in MEA recordings from *rd10* retina (A – C, and D – F).** (A) Typical unfiltered recording of neural activity from a *rd10* retina (age 12 months). (B) Spontaneous spiking activity obtained after high-pass filtering (300 Hz cut off frequency). Large amplitude spikes occurred in rhythmic bursts with interburst intervals of  $\sim 200$  ms. Short amplitude spikes (from a different cell) were fired more regularly. (C) Local field potentials (LFPs) obtained after low pass filtering (50 Hz cut off frequency). Oscillations with a frequency of around 5 Hz were observed. (D) Unfiltered recording from another *rd10* retina (age 9 months). (E) High-pass filtered recording with spike firing during the positive-going or flat part of the LFP. (F) Low pass filtered recording. doi:10.1371/journal.pone.0099075.g002

higher harmonics (Fig. S1). For this study, LFPs were recorded from retinæ of a total of 33 animals. Detailed results are provided in Table S1. In 9 animals aged 1 or 3 months, frequencies around 6 Hz were observed. In 24 animals aged from 4–12 months, frequencies around 4 Hz were observed. In our pharmacological experiments animal age was between 3 and 12 months. This means, that all rods and with few exceptions also cones had disappeared and remodelling as shown in Fig. 1 had taken place.

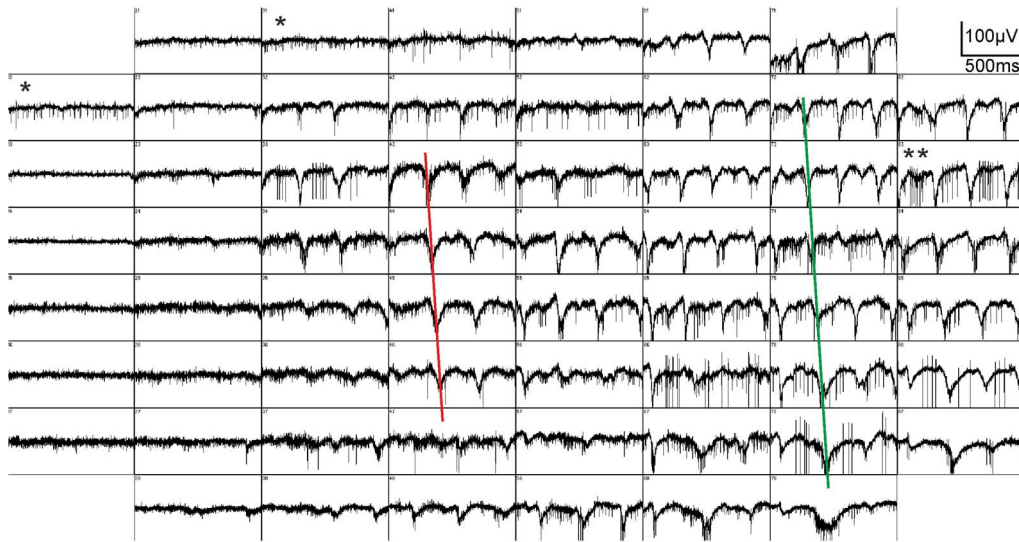
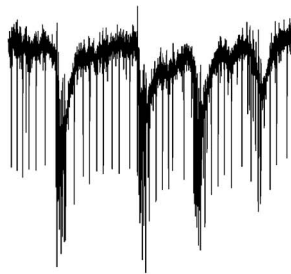
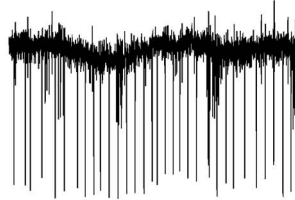
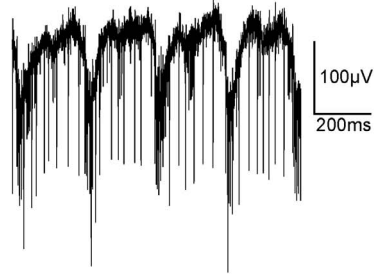
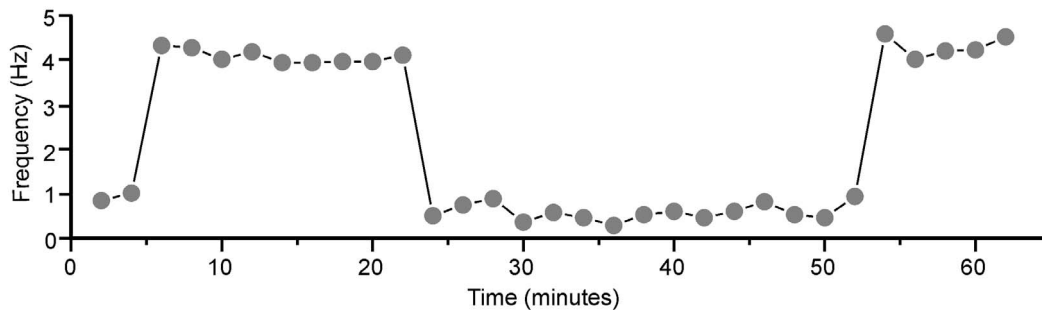
Spontaneous rhythmic activity has been reported for *rd1* and *rd10* by several studies. However, it is important to point out that oscillations are not always present. LFPs recorded in *rd10* retinæ varied considerably from retina to retina, from electrode to electrode within one retina and even within one electrode over time. Fig. 3A shows a recording from 60 electrodes in one retina (age of animal 9.5 months). The distance between the electrodes was 100  $\mu\text{m}$ . In several electrodes spikes were readily recorded, but no oscillations were observed (e.g. single asterisk). In most electrodes, however, strong oscillations could be recorded. Interestingly, the principal shape of the LFPs recorded at the different electrodes was very similar. Moreover, from upper to lower electrodes the phase of the LFPs seemed to be shifted. We marked the corresponding minima in the LFPs for electrodes 43 to 46 by a red line and for electrodes 72 to 77 by a green line. The two lines show the same slope. A simple way to interpret this phase shift is that the rhythmic activity is triggered at one site of the retina and then travels as a wave along the retina. By dividing the electrode distance by the time delay between the local minima at different electrodes we calculated the propagation velocity for the wave as 3.3 mm/s. This is slower than the velocity of wave propagation determined for *rd1* by Menzler and Zeck [17]. This

could either reflect a difference between *rd1* and *rd10* retinæ, or could depend on different recording conditions (experiments in our study were performed at room temperature, in the other study at 33–36°C).

LFPs recorded at one electrode could vary over time. Fig. 3B–D show recordings of electrode 83 (marked by two asterisks in Fig. 3A) taken 5, 30, or 60 min after the start of the experiment. In Fig. 3E the frequency of the oscillation obtained from the recording at this electrode was plotted over time for about one hour. Throughout the experiment, the retina was continuously superfused with oxygenized Ames solution without pharmacological agents at a constant rate. Oscillations were clearly visible for about 20 min (B, E), then vanished for about 30 min (C, E) and finally came back with a similar shape and frequency as observed during the first part of the experiment (D, E). These changes in the recording were not due to changes in the contact between electrodes and the retina, as ganglion cell spikes were recorded with the same amplitude at this electrode throughout the experiment. In summary, the results shown in Fig. 3 indicate that rhythmic electrical activity is not necessarily continuously generated but may depend on yet unknown physiological parameters.

### Rhythmic Electrical Activity Depends on Glutamatergic Input

The differences in the frequencies observed in LFPs from *rd1* and *rd10* retinæ could indicate that the mechanisms underlying the rhythmic activity differ in the two animal models. While the origin of the rhythmic activity in *rd1* has not been identified unequivocally, certain evidence suggests that bipolar cells and

**A Recording from 60 electrodes**

**B E83 after 5 min**

**C E83 after 30 min**

**D E83 after 60 min**

**E Frequency change at E83 over time**


**Figure 3. Spontaneous rhythmic electrical activity in *rd10* mouse retina can change.** (A) Activity recorded simultaneously from 60 electrodes in an 8x8 matrix (age of animal: 9.5 months). Oscillations were observed in the majority of channels along with spiking activity. Some channels showed no oscillations (e.g. indicated by single asterisk). The phase of the oscillation seemed to be shifted from upper rows to lower rows of electrodes as indicated by red and green lines. (B–E) Recording of electrode 83 (E83, marked by two asterisks in A) obtained over time. Oscillations were visible during the first 22 min (B), vanished for the next 30 min, while spiking activity remained (C), and finally came back with similar frequency and shape (D) as before. (E) Frequency plotted vs time.  
doi:10.1371/journal.pone.0099075.g003

amacrine cells may be involved. First, rhythmic changes in membrane potential were recorded from AII amacrine cells and from ON-cone bipolar cells in *rd1* mouse retina [14]. Second, oscillations as well as rhythmic spiking of ganglion cells were blocked by application of a mixture of the blockers for AMPA/kainate receptors and NMDA receptors CNQX and AP5

[12,14,15,17], indicating that glutamatergic excitation most probably from cone bipolar cells is involved in the generation of rhythmic activity. Finally, blockers of the two inhibitory transmitters glycine and GABA used by the vast majority of amacrine cells seemed to modulate rather than abolish rhythmic electrical activity [15,17]. In the following, we tested whether pharmacological

modulation of rhythmic electrical activity in *rd10* mice would differ from that observed in *rd1*.

Superfusion of the retina with a mixture of CNQX and DL-AP5 abolished LFPs in *rd10* retinæ in a reversible way (Fig. 4; age of animal 9 months). The recording in Fig. 4A shows rhythmic activity observed in the LFPs as well as spikes originating from two different cells. These spikes could be readily separated by conventional spike sorting algorithms (Fig. 4B). The spikes with the large amplitude were phase locked to the minima observed in LFPs, while the spikes with smaller amplitude were not. Upon application of CNQX/DL-AP5, oscillations in the LFPs were abolished (similar results were observed using CPP instead of DL-AP5, data not shown). Interestingly, the large amplitude spikes were also abolished while the small amplitude spikes remained. In a total of 9 experiments, we always observed that phase locked spikes vanished during application of CNQX/DL-AP5. In comparison to control recordings, remaining spike activity was on average reduced by 25%. Similar results were obtained in a total of 9 retinal pieces from 3 animals aged 7–9 months.

### Rhythmic Electrical Activity is Shaped by Inhibitory Input

Application of the glycine receptor blocker strychnine or the GABA<sub>A</sub> receptor blocker bicuculline alone hardly affected the spiking activity or the LFPs in *rd10* retinæ (data not shown). However, co-application of both blockers strongly changed the LFP pattern. The amplitude of the oscillation was on average increased 2–4 fold (total of 15 retinal pieces from 10 animals aged from 6.5–10 months). Sometimes the oscillatory signal saturated the amplifier of our MEA system. The frequency under control conditions ( $4.14 \pm 0.58$  Hz) was dramatically reduced to values of

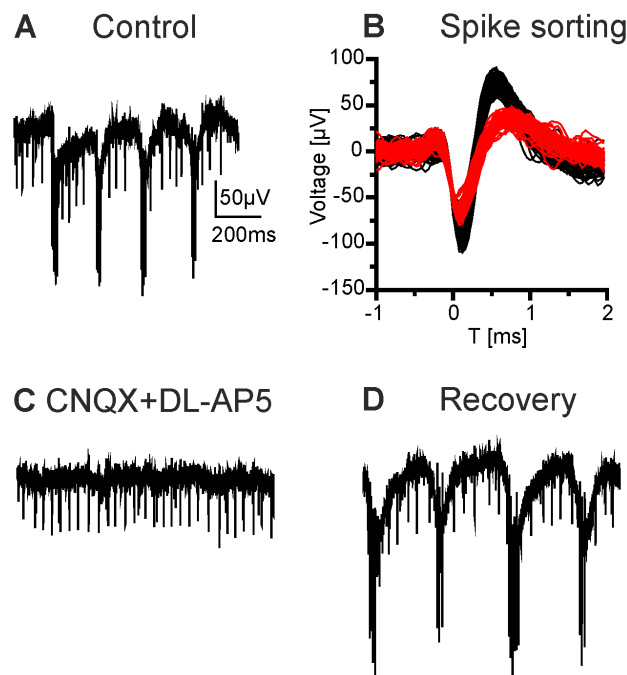


**Figure 4. Glutamate receptor blockers CNQX and DL-AP5 abolish rhythmic electrical activity.** (A) Unfiltered recording of an *rd10* retina displaying oscillations and spontaneous spiking activity (age 9 months). (B) Spike sorting of the recording shown in A. Spikes of two different amplitudes indicate activity from two ganglion cells. (C) Application of CNQX and DL-AP5 completely blocked the oscillations and bursts of large amplitude spikes. Small amplitude spikes remained unaffected. (D) The effect was reversible upon washout. doi:10.1371/journal.pone.0099075.g004

$0.95 \pm 0.3$  Hz. The effect was reversible upon washout of the blockers (Fig. 5A – C; age of animal 10 months).

Apart from glycine receptors and GABA<sub>A</sub> receptors, GABA<sub>B</sub> and GABA<sub>C</sub> receptors are also involved in synaptic inhibition in the retina [24–27]. Therefore, in a second set of experiments, we blocked all four inhibitory receptor types by a mixture of strychnine, bicuculline, CGP 54626, and TPMPA (Fig. 6; age of animal 12 months). Upon application of this cocktail, dramatic changes in the local field potentials occurred. The amplitude of the oscillation increased to values that partially saturated the amplifier (Fig. 6C). The frequency of the oscillation was reduced to values between 0.2 and 1 Hz. These effects were reversible upon washout (total of 9 retinal pieces from 8 animals aged 9–12 months). In wt retinæ, this cocktail of blockers did not induce spontaneous rhythmic activity as observed in *rd10* retinæ (data not shown). Blockade of glutamate receptors abolished the effect of the inhibitory blockers (Fig. 7; age of animal 9 months). The large fluctuations in the baseline observed during the inhibitory cocktail (Fig. 7B) were nearly absent during application of glutamate receptor blockers (Fig. 7C; 4 retinal pieces from 4 animals aged 9–12 months).

L-APB is an agonist at mGluR6, the metabotropic glutamate receptor present on both rod and cone ON-bipolar cells. L-APB hyperpolarizes ON-bipolar cells by starting a G-Protein dependent pathway that leads to the closure of cation channels, most likely TRPM1 [28–35]. If cone ON-bipolar cells are involved in the generation of rhythmic electrical activity, one might postulate that L-APB affects LFPs. Application of L-APB did not yield unequivocal results. In some cases, the LFP amplitude was slightly diminished. In most cases, however, L-APB affected neither amplitude nor frequency of the oscillations in a clear cut way (data not shown). This is probably due to lower expression of mGluR6 associated with the fact that during retinal remodelling mGluR6 becomes distributed over the somata and axons of bipolar cells (Fig. 1H) and may not effectively couple to its downstream signalling cascade [36].

### Rhythmic Electrical Activity in *rd10* Depends on Gap Junctions and is Modulated by HCN Channels

All amacrine cells are electrically coupled to each other and to cone ON-bipolar cells [37]. Application of the gap junction blocker MFA totally abolished spontaneous rhythmic activity in *rd1* retina [12,14,17,38]. We observed that this was also true for *rd10* retina (Fig. 8; age of animal 9.5 months; similar results were found in a total of 9 retinal pieces from 4 animals aged 9–10 months). Moreover, ganglion cell spiking was also totally abolished. Both effects were reversible upon washout (Fig. 8A – C). In the retina, all four isoforms of the hyperpolarization-activated and cyclic nucleotide-gated (HCN) channels that can function as pacemaker channels are expressed [39–42]. HCN channels, in particular when expressed in bipolar cells, might contribute to the rhythmic electrical activity observed in *rd1* retina [12] and *rd10* retina. We blocked HCN channels in two ways: by application of 3 mM Cs<sup>+</sup> (6 retinal pieces from 3 animals aged 9.5–10 months) and by application of ZD7288 (4 retinal pieces from 1 animal aged 9 months; data not shown). Both blockers affected spontaneous rhythmic activity in the same way: rhythmic activity persisted but the second harmonic frequency component disappeared while the basic frequency was reduced (Fig. 9A – C; age of animal 9.5 months). On average frequencies changed from  $4.65 \pm 0.51$  Hz under control conditions to  $2.78 \pm 0.69$  Hz during HCN channel blockage.

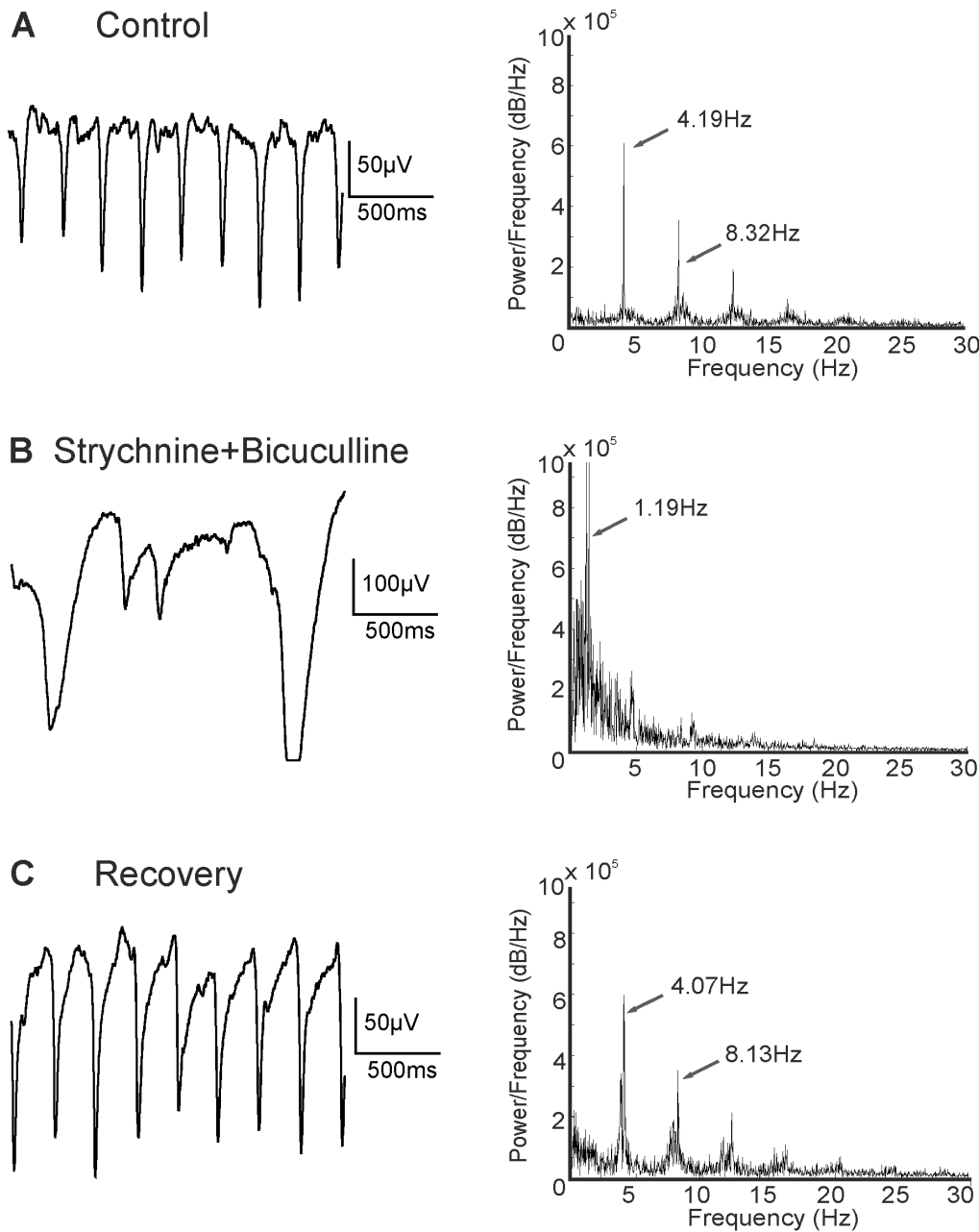


**Figure 5. Effects of strychnine and bicuculline on rhythmic electrical activity.** (A) Control recording (low pass filtered) displaying oscillations with a main frequency of  $\sim 4$  Hz (age 10 months). (B) Co-application of strychnine and bicuculline increased the LFP amplitude but reduced the frequency to  $\sim 1$  Hz. (C) The effect was fully reversible upon washout. doi:10.1371/journal.pone.0099075.g005

## Discussion

In the recent years, many studies have been performed on the retina of the *rd1* mouse, describing in detail the photoreceptor degeneration, the rewiring that takes place in the inner retina as well as changes in functional properties of retinal neurons [8,9]. However, as discussed earlier, due to the delayed and slower degeneration process, *rd10* may mimic human RP better than *rd1* and, therefore, may be a better model [10,11]. In both *rd1* and *rd10* retinæ spontaneous rhythmic activity was observed. Rhythms display frequencies of 10–16 Hz in *rd1*, but of 3–7 Hz in *rd10*. Most attempts to decipher the origin of spontaneous rhythmic activity were performed in *rd1* [12,14,15,17,43]. However, as *rd10*

is increasingly being used to study the process of retinal degeneration as well as a model to develop experimental therapies like stimulation of retinal ganglion cells by implants or by light-driven channels, it is important to understand the mechanisms underlying the spontaneous rhythmic activity. We, therefore, investigated whether the mechanisms suggested to elicit rhythmic activity in *rd1* also apply to *rd10*. We found, that despite the differences observed in the frequencies, the origin of rhythmic electrical activity in *rd1* and *rd10* seems to be quite similar.

In principle there are several possibilities how rhythmic activity could be generated. First, excitatory cells like bipolar cells might display endogenous rhythmic activity. Second, a continuous

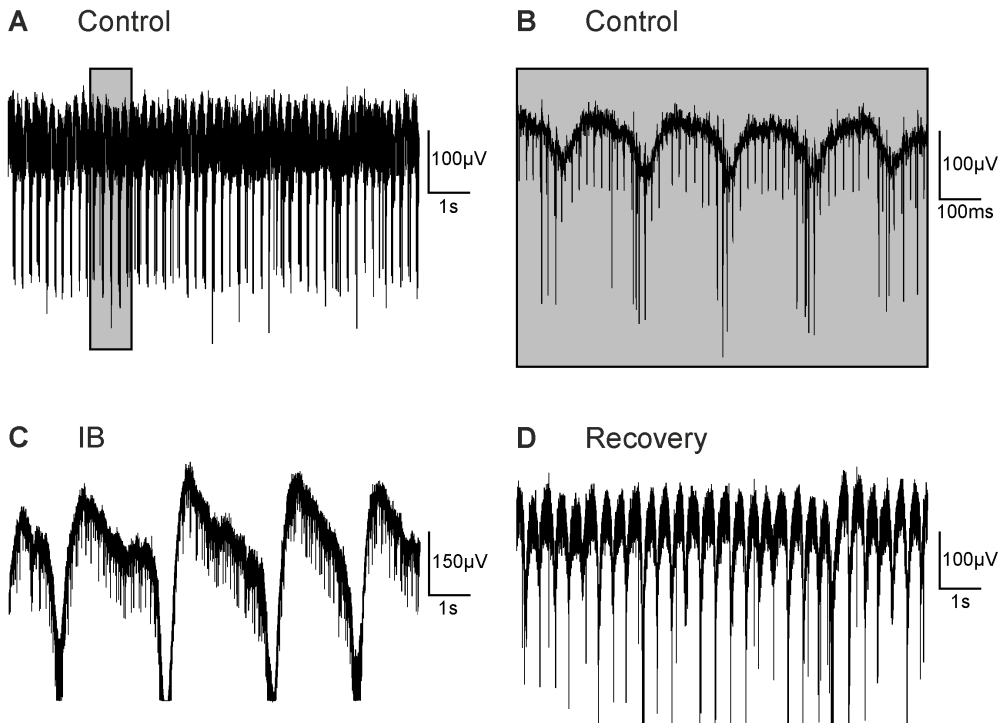


**Figure 6. Effect of inhibitory blockers on the LFPs.** (A) Unfiltered recording showing spontaneous spiking activity and oscillations (age 12 months). (B) A part of the recording from A (indicated by the grey box) at higher time resolution. (C) Co-application of strychnine, bicuculline, CGP 54626, and TPMPA (IB) reduced the frequency to around 0.4 Hz. The amplitude strongly increased, sometimes saturating the amplifier. (D) The effect was reversible upon washout. doi:10.1371/journal.pone.0099075.g006

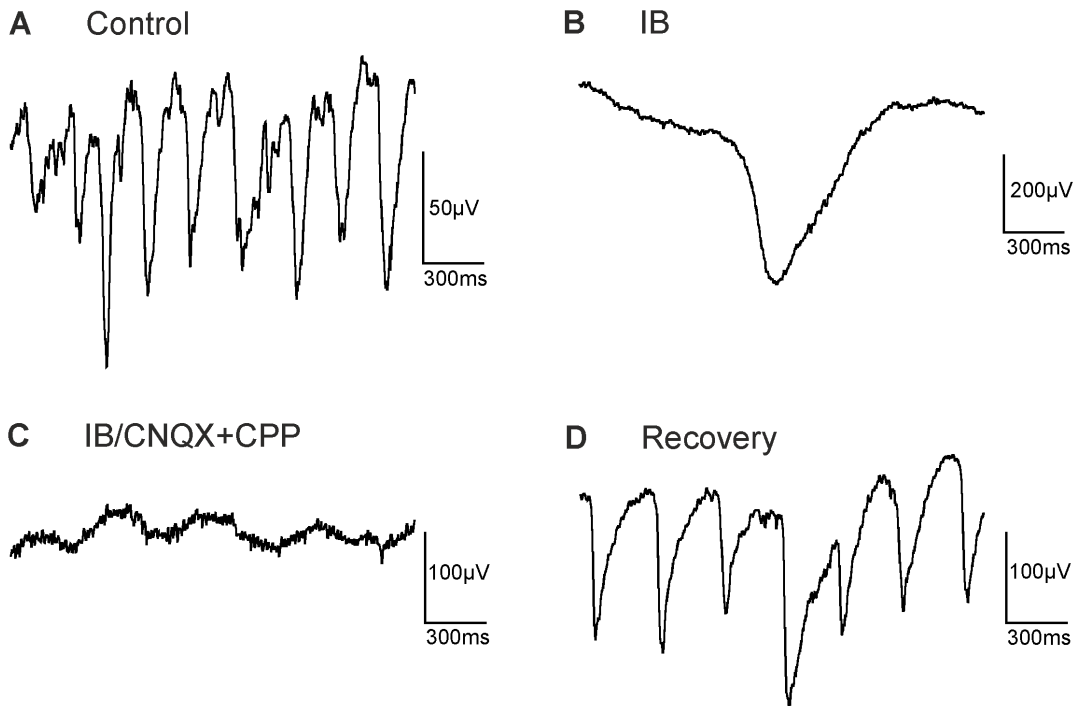


**Figure 7. Glutamate receptor blockers abolish baseline fluctuations induced by inhibitory blockers.** (A) Control recording (low pass filtered), showing LFPs with a frequency of ~4 Hz (age 9 months). (B) Upon application of inhibitory blockers (IB = strychnine, bicuculline, TPMPA, CGP 54626), the LFP frequency was reduced to below 1 Hz. Note the change in the amplitude scale. (C) Application of glutamate receptor blockers (CNQX and CPP) nearly abolished baseline fluctuations. (D) Upon washout of all agents typical oscillations of ~3 Hz were observed. doi:10.1371/journal.pone.0099075.g007



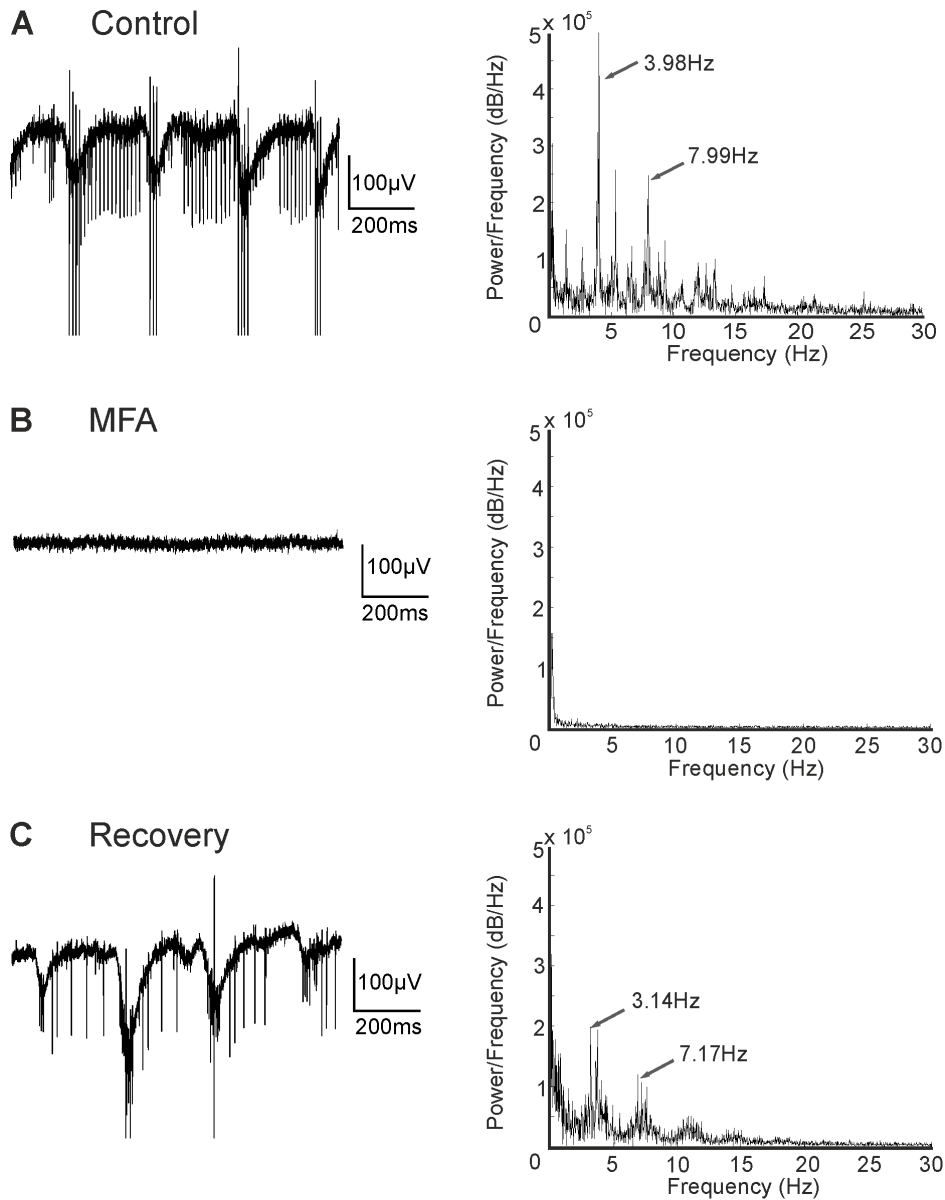


**Figure 8. The gap junction blocker MFA abolishes rhythmic electrical activity.** (A) Unfiltered baseline, showing spontaneous activity and LFPs with a frequency of  $\sim 4$  Hz (age 9.5 months). (B) Application of MFA blocked all spontaneous activity. (C) The effect was reversible upon washout.

doi:10.1371/journal.pone.0099075.g008

excitatory drive from bipolar cells could be modulated by inhibition that arises from rhythmic activity of amacrine cells. Indeed, spontaneous activity in several types of amacrine cells has been reported [44,45]. Finally, both mechanisms might contribute to rhythmic activity. We (Fig. 4) and others found that in both, *rd1* and *rd10*, blockage of ionotropic glutamate receptors abolishes oscillations, indicating that glutamatergic neurons – most likely bipolar cells – are a major drive for rhythmic activity [14,15,17]. In *rd10* we found that during blockade of glycinergic receptors and GABA<sub>A</sub> receptors oscillations persisted. However, the frequency was reduced to around 1 Hz while the amplitude of the oscillations was increased 2–4 fold. Additional blockage of GABA<sub>B</sub> and GABA<sub>C</sub> receptors further reduced the frequency to 0.2–1 Hz and increased the LFP amplitude. These results indicate that rhythmic activity in *rd10* arises even in the absence of inhibitory input and,

therefore, most likely originates from bipolar cell activity. Yet, inhibitory mechanisms modulate both frequency and amplitude of the oscillations. Blockade of ionotropic glutamate receptors abolishes the effects of inhibitory receptor blockers (Fig. 7). This might indicate that inhibitory receptor blockade acts presynaptically to the glutamate receptors, and hence on the bipolar cells. On the other hand, activity of amacrine cells seems to depend strongly on glutamatergic input [12,14]. In this case, inhibitory blockers would be without effect if glutamatergic input to amacrine cells is blocked.

For *rd1*, results with inhibitory blockers are less consistent. Menzler and Zeck [17] described an overall reduction in LFP frequency and an increase in LFP amplitude during application of bicuculline/strychnine, yet do not present numbers. Strychnine alone had a stronger effect than bicuculline. However, judging

from their Supplementary Fig. 2, strychnine barely changed the LFP frequency. Ye and Goo [15] found that strychnine and picrotoxin, another blocker of GABA<sub>A</sub> receptors, either alone or in combination increased the LFP amplitude 2–3 fold while the frequency was reduced to values around 4–5 Hz (as judged from their Fig. 4). This corresponds to a roughly twofold decrease in frequency in *rd1*, while in *rd10* frequency was reduced 3–5 fold in the presence of strychnine and bicuculline and even stronger if all inhibitory receptors were blocked (Fig. 6).

In recordings obtained from bipolar cells and AII amacrine cells of *rd1* retina, spontaneous oscillations in membrane potential were observed that strongly resembled rhythmic activity recorded using MEAs [12,14]. The authors suggest that rhythmic activity originates from the tight interaction between ON-cone bipolar cells and AII amacrine cells. AII amacrine cells contact ON-cone bipolar cells via electrical synapses in form of gap junctions [46–50]. In fact, MFA that was shown to block gap junctions in the retina [51,52] abolished oscillations in both *rd1* [12,14,17] and *rd10* (present study; [38]). Interestingly, ON-bipolar cells express hyperpolarization-activated and cyclic nucleotide-gated (HCN) channels [39–42]. In several systems, HCN channels function as pacemaker channels [53,54] and could, therefore, be the source of spontaneous rhythmic activity in ON-bipolar cells. However, blocking HCN channels using either Cs<sup>+</sup> or ZD7288 did not abolish oscillations in the membrane potential of ON-cone bipolar cells in *rd1* retinæ [12]. HCN channel blockers reduced the frequency from 10 Hz to around 6 Hz, but increased the power at the peak oscillatory frequency by more than 700%. We did not observe such an increase in power in *rd10* retinæ. In *rd10*, Cs<sup>+</sup> and ZD7288 mostly reduced the second peak of the power spectrum but only slightly changed the frequency of the first peak (Fig. 9).

In summary, despite the differences in the process of degeneration and the different frequencies of spontaneous rhythmic activity in *rd1* and *rd10*, we only found small differences in the pharmacological modulation of rhythmic activity in both models. This indicates that the cellular origin of the spontaneous activity may be quite similar in *rd1* and *rd10*. Could the difference in frequencies between *rd1* and *rd10* be attributed to different genetic backgrounds? We found that in *rd10* the frequency observed in LFP oscillation is modulated by a variety of ion channels, amongst them HCN channels, glycine receptors, and GABA receptors. Differences in the expression level of any of these channels between mice of different backgrounds might, therefore, affect the frequency of the oscillations. Our animals carried the *rd10* mutation in a C57BL/6 background. Trenholm and colleagues recorded oscillations in the membrane potential of AII amacrine cells and ON-cone bipolar cells in retinal slices from animals carrying the *rd1* mutation in the same background. They found frequencies of around 15 Hz (see e.g. their Fig. 1) [12]. These values are very different from those obtained in the present study for *rd10*, but consistent with data obtained by the same authors from animals carrying the *rd1* mutation in a different genetic background and with previous reports on *rd1* retinæ using MEA recordings [13–16,55].

We (Fig. 3) and others provided evidence that rhythmic electrical activity might spread across the retina in form of a wave [17]. This is reminiscent of waves of retinal activity observed during the early postnatal period before eye opening (e.g. [56,57]) and of the propagation of electrical excitation in the heart. It is not entirely clear why spontaneous activity originating at one spot in the retina should dominate oscillations over a larger retinal area, but once generated the pacemaker wave could easily spread across the retina through the gap junctional network between the AII amacrine cells [37]. Further studies will have to identify the

mechanism underlying the generation of such waves and will have to address the question why robust spontaneous activity disappears entirely for longer time and comes back (Fig. 3).

Why does spontaneous rhythmic activity originate at all in the retina of *rd1* and *rd10* mice? Spontaneous rhythmic activity could result from substantial remodelling and rewiring processes described in retinal tissue upon photoreceptor degeneration. Such processes could transform the retina into a self-signalling neuronal network [6–10,58]. Moreover, several lines of evidence suggest that changes of the functional properties of bipolar cells occur at early stages of degeneration when photoreceptors are still present and long before substantial remodelling has taken place. These changes include the aberrant expression of ionotropic glutamate receptors and the loss of expression or reduced activation of metabotropic glutamate receptors on ON-bipolar cells as well as the increase of GABA mediated currents [3,6,24,36,59,60]. Such changes could explain why oscillations can be observed in *rd10* mice at postnatal week 2, when photoreceptors are still present and no remodelling has occurred [61]. On the other hand, there is evidence that rhythmic activity in the retina does not depend on complex rewiring processes or degeneration-induced changes of bipolar cell physiology. Trenholm et al. [12] reported that in wild type retina, blockage of photoreceptor input by application of NBQX and APB induces membrane oscillations in both ON-cone bipolar cells and AII amacrine cells similar to those observed in *rd1* retina. This would suggest that the lack of photoreceptor input is sufficient to trigger oscillations in the retina. Clearly, while over the last years we have gained considerable insight into the process of retinal degeneration, several important issues still need clarification in further studies.

## Materials and Methods

### Animals

Wildtype animals of the strain C57BL/6 were obtained from Charles River. *Rd10* mice were bred locally from breeding pairs obtained from Jackson (strain name: B6.CXBX1-*Pde6b*<sup>rd10</sup>/J). In this line the *rd10* mutation was backcrossed onto the C57BL/6J background for 5 generations before intercrossing to homozygosity. All animals were kept on a 12 h light/dark cycle with food and water ad libitum. All experiments were performed in accordance with the German Law for the Protection of Animals and after approval was obtained by the regulatory authorities, the Forschungszentrum Jülich and the Landesamt für Natur, Umwelt und Verbraucherschutz of the land North-Rhine Westfalia.

### Immunohistochemistry

For immunohistochemistry, animals were deeply anesthetized with isoflurane and killed by decapitation. The eyes were enucleated and opened by an encircling cut at the limbus. The retinæ in the eyecup were immersion-fixed for 30 min in 4% paraformaldehyde (PA) in 0.1 M phosphate buffer (PB; pH 7.4) at room temperature and washed in PB several times. Tissue was incubated in 10% sucrose in PB for 1 h, followed by 30% sucrose in PB overnight. The retina was flat embedded and frozen in optimal cutting temperature (OCT) compound (NEG-50, Richard Allen Scientific, Thermo Fisher Scientific, Germany). Vertical sections (i.e. perpendicular to the retinal layers, 20 µm thick) were cut on a cryostat (HM 560 CryoStar; MICROM; Walldorf; Germany) and collected on Superfrost Plus slides (Menzel, Braunschweig, Germany). Sections were pre-treated with blocking solution (5% Chemiblocker (Chemicon, Hofheim, Germany), 0.5% Triton-X100, 0.05% NaN<sub>3</sub> in PB) for 1 hour, followed by incubation with primary antibodies over night, diluted in the same

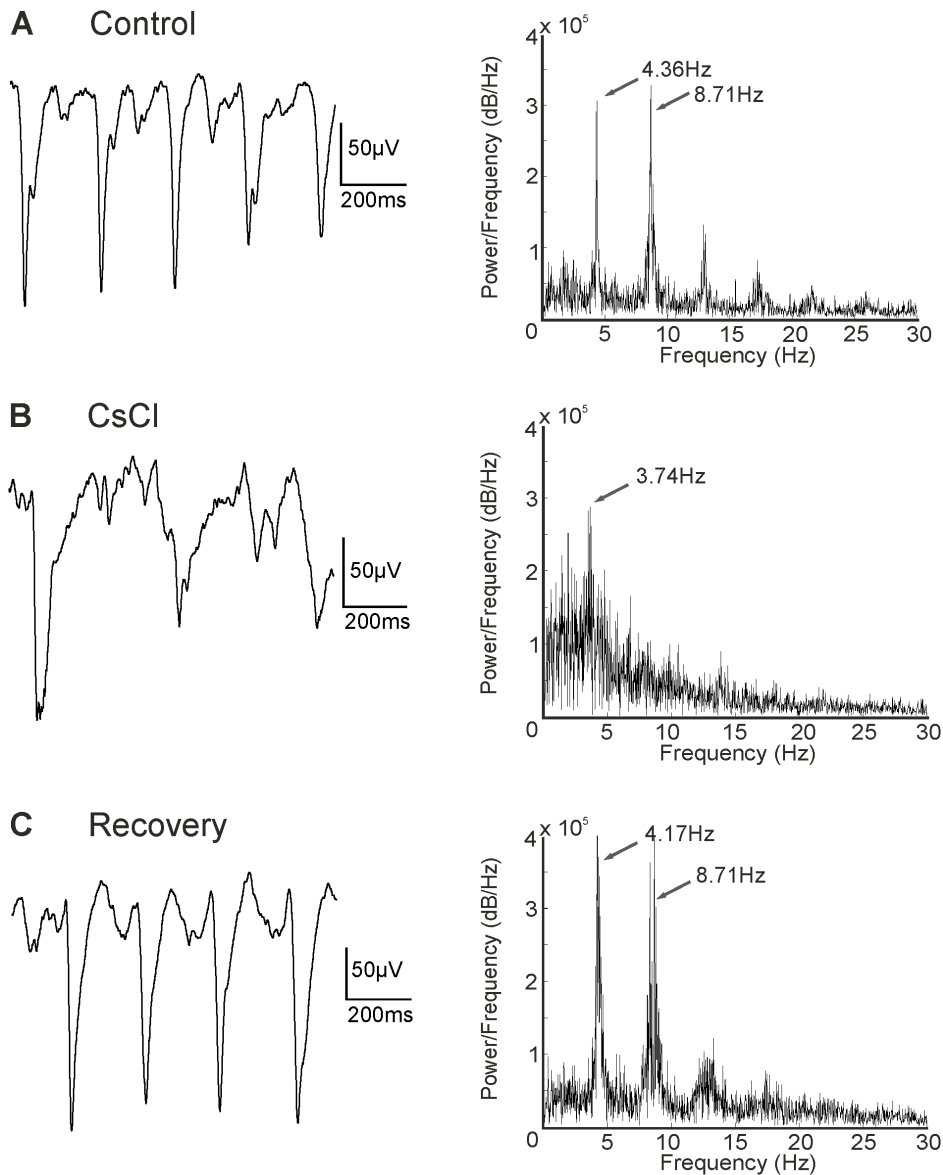


**Figure 9. HCN channel blocker reduces rhythmic electrical activity.** (A) Low pass filtered recording, frequency  $\sim 4$  Hz (age 9.5 months). (B) Blocking HCN channels with CsCl abolished the second harmonic peak and slightly reduced the frequency of the first peak. (C) Recovery. doi:10.1371/journal.pone.0099075.g009

solution. Sections were washed in PB and incubated in secondary antibodies diluted in 5% Chemiblocker, 0.5% Triton-X100 in PB for 1 h, washed in PB and coverslipped with Aqua Polymount (Polysciences, Eppelheim, Germany). Sections were examined with a confocal laser scanning microscope (Leica TCS SP5, Leica Microsystems, Heidelberg, Germany) with 63x/1.4 oil immersion lenses. Images were processed and printed with Adobe Photoshop. Primary antibodies included AB5585 (anti-recoverin polyclonal antibody, raised in rabbit, 1:2000, Chemicon, Germany); AB5405 (anti-opsin red/green, raised in rabbit, 1:800, Chemicon, Germany); PKC $\alpha$  (anti-protein kinase C $\alpha$ , raised in rabbit, 1:4000; Santa Cruz Biotechnology, Inc.); mGluR6 (anti-GRM6, raised in rabbit, 1:1000, Sigma, Germany); CabP (anti-calbindin 28k, raised in mouse, 1:1000, Sigma, Germany). Secondary antibodies included donkey anti-rabbit Cy2 (1:400, Dianova, Germany), donkey anti-rabbit Cy3 (1:500, Dianova, Germany), goat anti-

rabbit A488 (1:500, Invitrogen, Germany), and donkey anti-mouse Cy3 (1:100, Dianova, Germany).

### Multi-electrode Arrays (MEA) and Data Recording

3D MEAs containing 60 platinum electrodes (conical shape, diameter: 30  $\mu\text{m}$  or 40  $\mu\text{m}$ ) on a glass substrate (Qwane Biosciences, Lausanne, Switzerland) with 8x8 matrix without corner electrodes, were used for recording of local field potentials (LFP) and spiking activities from ganglion cells. Spacing between electrodes was either 100  $\mu\text{m}$  or 200  $\mu\text{m}$ . Impedances of the electrodes were 600–900 k $\Omega$  ( $\varnothing$  30  $\mu\text{m}$ ) and 250–450 k $\Omega$  ( $\varnothing$  40  $\mu\text{m}$ ). The MEA60 data acquisition system (MC\_Card, Multichannel system, Reutlingen, Germany) consisted of a RS-232 interface, an integrated preamplifier and MEA 1060 bandpass filter (amplification gain: 1200), and a personal computer. The waveforms were recorded with the sampling frequency rate of 25 kHz/channel. The data were later converted to ASCII files by

MC\_Data for further analysis with OriginPro8 and by custom made MATLAB scripts.

### Tissue Preparation

Retinae of wild type (adult) and *rd 10* (postnatal day 30–12 months) mice were prepared for MEA recordings. Briefly, the mouse was deeply anesthetized with isoflurane and killed by decapitation. The eyeballs were enucleated and retinae were isolated. The retinae were cut into two halves and one half was mounted with ganglion cells towards the electrode side of the MEA. MEAs were pre-treated in a plasma cleaner (Diener Electronic GmbH+Co. KG, Germany) and coated with Poly-D-lysine hydrobromide (PDL, Sigma, Germany). The retinal preparation was maintained in carbonate-buffered AMES solution, bubbled with 95% O<sub>2</sub>+5% CO<sub>2</sub> at a pH of ~7.4. All pharmacological agents were dissolved in oxygenated AMES buffer and delivered to the retina by continuous perfusion at a flow rate of 3 ml/min. All results shown are from experiments performed at room temperature (RT). Oscillations at RT (4–6 Hz) were similar to those found in own preliminary experiments carried out at 32°C (5–7 Hz) and to those reported for *rd10* at 32°C (4–7 Hz) [16]. However, in our hands, recordings at RT showed more stable oscillations and were, therefore, chosen for the long lasting recordings performed in this study.

### Pharmacology

The following pharmacological agents were used to study the origin of intrinsic neuronal oscillations: L-(+)-2-Amino-4-phosphonobutyric acid (L-APB), 100 μM, agonist at mGLUR6; 6-cyano-2,3-dihydroxy-7-nitro-quinoxaline-2,3-dione disodium (CNQX), 20 μM, AMPA/kainate receptor antagonist; DL-2-Amino-5-phosphonopentanoic acid (DL-AP5), 50 μM, NMDA receptor antagonist (D-AP5 is a strong NMDA receptor antagonist, while L-AP5 has been reported to be a weak agonist at glutamate receptors; we found no difference in the effect of the mixtures CNQX/DL-AP5 and CNQX/R-CPP, respectively); 3-((R)-2-Carboxypiperazin-4-yl)-propyl-1-phosphonic acid (R-CPP), 40 μM, NMDA receptor antagonist; strychnine, 10 μM, glycine receptor antagonist; bicuculline, 30 μM, GABA<sub>A</sub> receptor antag-

onist; [S-(R\*,R\*)]-[3-[[1-(3,4-Dichlorophenyl)ethyl]amino]-2-hydroxypropyl](cyclohexylmethyl) phosphinic acid (CGP 54626), 2 μM, GABA<sub>B</sub> receptor antagonist; 1,2,5,6-Tetrahydropyridin-4-yl)methylphosphinic acid (TPMPA), 100 μM, GABA<sub>C</sub> receptor antagonist; meclofenamic acid (MFA), 100 μM, gap junction blocker; cesium chloride (CsCl), 3 mM, HCN channel blocker, and 4-Ethylphenylamino-1,2-dimethyl-6-methylaminopyrimidinium chloride (ZD7288), 100 μM, HCN channel blocker.

### Supporting Information

**Figure S1 Different frequencies can be observed in LFP oscillations in *rd10*.** Unfiltered recordings of different *rd 10* retinae (left) with Fast Fourier Transformations (FFT; right). (A) Main frequency at ~3 Hz with a second harmonic frequency at ~6 Hz (age 12 months). (B) Main frequency at ~5 Hz and second peak at ~10 Hz (age 8 months). (TIF)

**Table S1 Frequencies observed in LFP oscillations in *rd10*.** Experiments were performed on a total of 33 animals ranging from 1–12 months. The group aged 9 months also includes the animals aged 9.5 months. The frequency of oscillations was slightly higher in animals between 1 and 3 months. In animals aged 4–12 months, little variation in the frequency was observed. Frequency is given as mean ± standard deviation (SD). (DOCX)

### Acknowledgments

We thank Christoph Aretzweiler for great technical assistance in immunohistochemistry and MEA recording and Dr. Johnny Hendriks for help in the evaluation of MEA recordings.

### Author Contributions

Conceived and designed the experiments: SB CH AM GT PW FM. Performed the experiments: SB CH AM. Analyzed the data: SB CH AM GT PW FM. Wrote the paper: SB FM.

### References

- Bowes C, Li T, Danciger M, Baxter LC, Applebury ML, et al. (1990) Retinal degeneration in the *rd* mouse is caused by a defect in the beta subunit of rod cGMP-phosphodiesterase. *Nature* 347: 677–680.
- Chang B, Hawes NL, Hurd RE, Davisson MT, Nusinowitz S, et al. (2002) Retinal degeneration mutants in the mouse. *Vision Res* 42: 517–525.
- Strettoi E, Pignatelli V (2000) Modifications of retinal neurons in a mouse model of retinitis pigmentosa. *Proc Natl Acad Sci U S A* 97: 11020–11025.
- Carter-Dawson LD, LaVail MM, Sidman RL (1978) Differential effect of the *rd* mutation on rods and cones in the mouse retina. *Invest Ophthalmol Vis Sci* 17: 489–498.
- Blanks JC, Adinolfi AM, Lolley RN (1974) Photoreceptor degeneration and synaptogenesis in retinal-degenerative (*rd*) mice. *J Comp Neurol* 156: 95–106.
- Marc RE, Jones BW, Anderson JR, Kinard K, Marshak DW, et al. (2007) Neural reprogramming in retinal degeneration. *Invest Ophthalmol Vis Sci* 48: 3364–3371.
- Marc RE, Jones BW, Watt CB, Strettoi E (2003) Neural remodeling in retinal degeneration. *Prog Retin Eye Res* 22: 607–655.
- Strettoi E, Porciatti V, Falsini B, Pignatelli V, Rossi C (2002) Morphological and functional abnormalities in the inner retina of the *rd/rd* mouse. *J Neurosci* 22: 5492–5504.
- Strettoi E, Pignatelli V, Rossi C, Porciatti V, Falsini B (2003) Remodeling of second-order neurons in the retina of *rd/rd* mutant mice. *Vision Res* 43: 867–877.
- Phillips MJ, Otteson DC, Sherry DM (2010) Progression of neuronal and synaptic remodeling in the *rd10* mouse model of retinitis pigmentosa. *J Comp Neurol* 518: 2071–2089.
- Gargini C, Terzibasi E, Mazzoni F, Strettoi E (2007) Retinal organization in the retinal degeneration 10 (*rd10*) mutant mouse: a morphological and ERG study. *J Comp Neurol* 500: 222–238.
- Trenholm S, Borowska J, Zhang J, Hoggarth A, Johnson K, et al. (2012) Intrinsic oscillatory activity arising within the electrically coupled AII amacrine-ON cone bipolar cell network is driven by voltage-gated Na<sup>+</sup> channels. *J Physiol* 590: 2501–2517.
- Margolis DJ, Newkirk G, Euler T, Detwiler PB (2008) Functional stability of retinal ganglion cells after degeneration-induced changes in synaptic input. *J Neurosci* 28: 6526–6536.
- Borowska J, Trenholm S, Awatramani GB (2011) An intrinsic neural oscillator in the degenerating mouse retina. *J Neurosci* 31: 5000–5012.
- Ye JH, Goo YS (2007) The slow wave component of retinal activity in *rd/rd* mice recorded with a multi-electrode array. *Physiol Meas* 28: 1079–1088.
- Goo YS, Ahn KN, Song YJ, Ahn SH, Han SK, et al. (2011) Spontaneous Oscillatory Rhythm in Retinal Activities of Two Retinal Degeneration (*rd1* and *rd10*) Mice. *Korean J Physiol Pharmacol* 15: 415–422.
- Menzler J, Zeck G (2011) Network oscillations in rod-degenerated mouse retinas. *J Neurosci* 31: 2280–2291.
- Haverkamp S, Ghosh KK, Hirano AA, Wässle H (2003) Immunocytochemical description of five bipolar cell types of the mouse retina. *J Comp Neurol* 455: 463–476.
- Nomura A, Shigemoto R, Nakamura Y, Okamoto N, Mizuno N, et al. (1994) Developmentally regulated postsynaptic localization of a metabotropic glutamate receptor in rat rod bipolar cells. *Cell* 77: 361–369.
- Mataruga A, Kremmer E, Müller F (2007) Type 3a and type 3b OFF cone bipolar cells provide for the alternative rod pathway in the mouse retina. *J Comp Neurol* 502: 1123–1137.
- Peichl L, Gonzalez-Soriano J (1994) Morphological types of horizontal cell in rodent retinae: a comparison of rat, mouse, gerbil, and guinea pig. *Vis Neurosci* 11: 501–517.

22. Haverkamp S, Wässle H (2000) Immunocytochemical analysis of the mouse retina. *J Comp Neurol* 424: 1–23.
23. Ye JH, Kim KH, Goo YS (2008) Comparison of electrically-evoked ganglion cell responses in normal and degenerate retina. *Conf Proc IEEE Eng Med Biol Soc* 2008: 2465–2468.
24. Varela C, Igartua I, De la Rosa EJ, De la Villa P (2003) Functional modifications in rod bipolar cells in a mouse model of retinitis pigmentosa. *Vision Res* 43: 879–885.
25. Farajian R, Pan F, Akopian A, Volgyi B, Bloomfield SA (2011) Masked excitatory crosstalk between the ON and OFF visual pathways in the mammalian retina. *J Physiol* 589: 4473–4489.
26. Enz R, Bormann J (1995) Expression of glycine receptor subunits and gephyrin in single bipolar cells of the rat retina. *Vis Neurosci* 12: 501–507.
27. Müller F, Boos R, Wässle H (1992) Actions of GABAergic ligands on brisk ganglion cells in the cat retina. *Vis Neurosci* 9: 415–425.
28. Dhingra A, Fina ME, Neinstein A, Ramsey DJ, Xu Y, et al. (2011) Autoantibodies in melanoma-associated retinopathy target TRPM1 cation channels of retinal ON bipolar cells. *J Neurosci* 31: 3962–3967.
29. Krizaj D, Huang W, Furukawa T, Punzo C, Xing W (2010) Plasticity of TRPM1 expression and localization in the wild type and degenerating mouse retina. *Vision Res* 50: 2460–2465.
30. Koike C, Obara T, Uriu Y, Numata T, Sanuki R, et al. (2010) TRPM1 is a component of the retinal ON bipolar cell transduction channel in the mGluR6 cascade. *Proc Natl Acad Sci U S A* 107: 332–337.
31. Koike C, Numata T, Ueda H, Mori Y, Furukawa T (2010) TRPM1: a vertebrate TRP channel responsible for retinal ON bipolar function. *Cell Calcium* 48: 95–101.
32. Nakamura M, Sanuki R, Yasuma TR, Onishi A, Nishiguchi KM, et al. (2010) TRPM1 mutations are associated with the complete form of congenital stationary night blindness. *Mol Vis* 16: 425–437.
33. Morgans CW, Brown RL, Duvoisin RM (2010) TRPM1: the endpoint of the mGluR6 signal transduction cascade in retinal ON-bipolar cells. *Bioessays* 32: 609–614.
34. Kaur T, Nawy S (2012) Characterization of *Trpm1* desensitization in ON bipolar cells and its role in downstream signalling. *J Physiol* 590: 179–192.
35. Slaughter MM, Miller RF (1981) 2-amino-4-phosphonobutyric acid: a new pharmacological tool for retina research. *Science* 211: 182–185.
36. Puthussery T, Gayet-Primo J, Pandey S, Duvoisin RM, Taylor WR (2009) Differential loss and preservation of glutamate receptor function in bipolar cells in the *rd10* mouse model of retinitis pigmentosa. *Eur J Neurosci* 29: 1533–1542.
37. Kolb H, Famiglietti EV (1974) Rod and cone pathways in the inner plexiform layer of cat retina. *Science* 186: 47–49.
38. Toychiev AH, Ivanova E, Yee CW, Sagdullaev BT (2013) Block of gap junctions eliminates aberrant activity and restores light responses during retinal degeneration. *J Neurosci* 33: 13972–13977.
39. Fyk-Kolodziej B, Pourcho RG (2007) Differential distribution of hyperpolarization-activated and cyclic nucleotide-gated channels in cone bipolar cells of the rat retina. *J Comp Neurol* 501: 891–903.
40. Müller F, Scholten A, Ivanova E, Haverkamp S, Kremmer E, et al. (2003) HCN channels are expressed differentially in retinal bipolar cells and concentrated at synaptic terminals. *Eur J Neurosci* 17: 2084–2096.
41. Ivanova E, Müller F (2006) Retinal bipolar cell types differ in their inventory of ion channels. *Vis Neurosci* 23: 143–154.
42. Knop GC, Seeliger MW, Thiel F, Mataruga A, Kaupp UB, et al. (2008) Light responses in the mouse retina are prolonged upon targeted deletion of the HCN1 channel gene. *Eur J Neurosci* 28: 2221–2230.
43. Goo YS, Ye JH, Lee S, Nam Y, Ryu SB, et al. (2011) Retinal ganglion cell responses to voltage and current stimulation in wild-type and *rd1* mouse retinas. *J Neural Eng* 8: 035003.
44. Petit-Jacques J, Volgyi B, Rudy B, Bloomfield S (2005) Spontaneous oscillatory activity of starburst amacrine cells in the mouse retina. *J Neurophysiol* 94: 1770–1780.
45. Feigenspan A, Gustincich S, Bean BP, Raviola E (1998) Spontaneous activity of solitary dopaminergic cells of the retina. *J Neurosci* 18: 6776–6789.
46. Deans MR, Volgyi B, Goodenough DA, Bloomfield SA, Paul DL (2002) Connexin36 is essential for transmission of rod-mediated visual signals in the mammalian retina. *Neuron* 36: 703–712.
47. Tsukamoto Y, Morigiwa K, Ueda M, Sterling P (2001) Microcircuits for night vision in mouse retina. *J Neurosci* 21: 8616–8623.
48. Trexler EB, Li W, Massey SC (2005) Simultaneous contribution of two rod pathways to AII amacrine and cone bipolar cell light responses. *J Neurophysiol* 93: 1476–1485.
49. Famiglietti EV Jr., Kolb H (1975) A bistratified amacrine cell and synaptic circuitry in the inner plexiform layer of the retina. *Brain Res* 84: 293–300.
50. Kolb H, Nelson R (1983) Rod pathways in the retina of the cat. *Vision Res* 23: 301–312.
51. Veruki ML, Hartveit E (2009) Meclofenamic acid blocks electrical synapses of retinal AII amacrine and on-cone bipolar cells. *J Neurophysiol* 101: 2339–2347.
52. Pan F, Mills SL, Massey SC (2007) Screening of gap junction antagonists on dye coupling in the rabbit retina. *Vis Neurosci* 24: 609–618.
53. DiFrancesco D (1981) A study of the ionic nature of the pace-maker current in calf Purkinje fibres. *J Physiol* 314: 377–393.
54. Kaupp UB, Seifert R (2001) Molecular diversity of pacemaker ion channels. *Annu Rev Physiol* 63: 235–257.
55. Stasheff SF (2008) Emergence of sustained spontaneous hyperactivity and temporary preservation of OFF responses in ganglion cells of the retinal degeneration (*rd1*) mouse. *J Neurophysiol* 99: 1408–1421.
56. Feller MB, Butts DA, Aaron HL, Rokhsar DS, Shatz CJ (1997) Dynamic processes shape spatiotemporal properties of retinal waves. *Neuron* 19: 293–306.
57. Wong RO (1999) Retinal waves and visual system development. *Annu Rev Neurosci* 22: 29–47.
58. Jones BW, Kondo M, Terasaki H, Lin Y, McCall M, et al. (2012) Retinal remodeling. *Jpn J Ophthalmol* 56: 289–306.
59. Chua J, Fletcher EL, Kalloniatis M (2009) Functional remodeling of glutamate receptors by inner retinal neurons occurs from an early stage of retinal degeneration. *J Comp Neurol* 514: 473–491.
60. Lin Y, Jones BW, Liu A, Vazquez-Chona FR, Lauritzen JS, et al. (2012) Rapid glutamate receptor 2 trafficking during retinal degeneration. *Mol Neurodegeneration* 7: 7–21.
61. Jae SA, Ahn KN, Kim JY, Seo JH, Kim HK, et al. (2013) Electrophysiological and Histologic Evaluation of the Time Course of Retinal Degeneration in the *rd10* Mouse Model of Retinitis Pigmentosa. *Korean J Physiol Pharmacol* 17: 229–235.